

SOLAR ACTIVITY AND CURRENT SHEET FORMATION ABOVE A BIPOLAR ACTIVE REGION

I.M. Podgorny¹ and A.I. Podgorny²

¹Institute for Astronomy RAN, Moscow, Russia, podgorny@inasan.rssi.ru

²Lebedev Physical Institute, Moscow, Russia

Abstract. Current sheet (CS) formation and energy accumulation for a solar flare above a bipolar region is demonstrated in a numerical MHD experiment. The Peresvet code is applied to solve the system of dissipative MHD equations. It is shown that CS is formed at the border between the old magnetic flux and new one when the magnetic fields are oppositely directed. The energy accumulated in the CS can be rapidly released producing a solar flare. In other part of the border, where the magnetic fluxes have the same direction, a front of high-density plasma develops. The front moves with the velocity equal to a half of the sound speed, while the CS is displaced only a little becoming the vertical one.

The general cycle of solar activity

The most popular index of solar activity is the Wolf index $W = 10g + f$, where g is the number of solar spot groups, f is the number of solar spots. The time dependence of W reveals a periodical structure with a period of 11.2 years (Fig. 1). Maximum probabilities P of solar flare occurrence are located not exactly at W_{\max} , but are shifted to the right and to the left of it. This phenomenon is known as a Gnevishhev gap. The Gnevishhev gap implies that flare occurrence probability may depend not only on spot number proper but also on the rate of spot number variation, i.e. $P \sim f \, df/dt$. Such dependence is consistent with the idea that a solar flare is produced due to decay of the CS above an active region, because for CS creation it is necessary to have several spots in an active region and magnetic field variations on the photosphere, which produce magnetic disturbances in the corona (Podgorny and Podgorny, 1992, 2002).

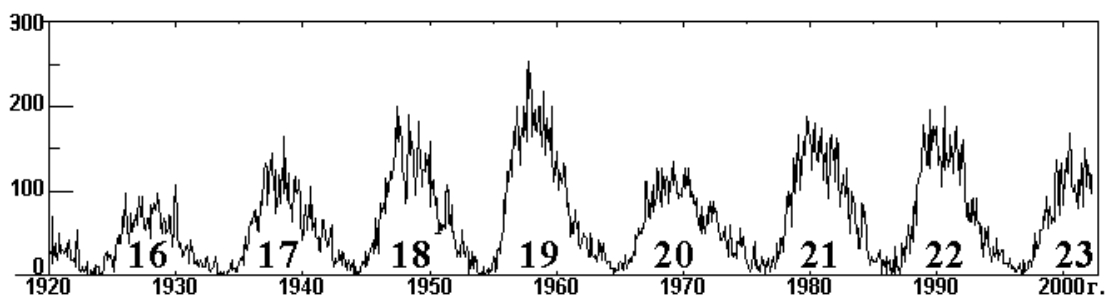


Fig. 1. Cycles of solar activity

Solar flare activity is strongly associated with solar global magnetic field. At activity minimum the Sun has the poloidal (dipole) magnetic field and there are no Sun spots in this period. An increase in W is accompanied by dipole magnetic field disappearance and generation of toroidal magnetic field inside the Sun. This phenomenon is associated with a differential solar rotation, the angular velocity being maximum on the equator. Differential solar rotation bends a magnetic field line, so that a dipole line becomes a toroidal one. The maximum of the toroidal magnetic field coincides with the maximum of W . Then, the toroidal field decreases and drops to zero in 11.2 years at next W_{\min} . The scheme of solar global magnetic field periodic change is shown in Fig. 2. In next 11.2 year the initial magnetic field configuration is restored, but with the reversal dipole field. It is more correct to say about $11.2 \times 2 = 22.4$ year cycle.

The active regions are rotating together with the Sun. The important feature of active regions is distribution of spot polarities. In one hemisphere the leading spots (those moving ahead) of all active regions possess the same polarity of the magnetic field, while all the rear spots have the opposite polarity. In the other hemisphere the leading and rear spots have polarities that are opposite to the polarities in the first hemisphere. In next 11.2-year cycle, a similar picture of spot distribution appears, but the magnetic fields of leading and rear spots change their polarity. The observed regularity is explained by spots creation due to flowing up parts of strong magnetic tubes of the toroidal magnetic field from the photosphere. As a result, arch magnetic configurations are formed.

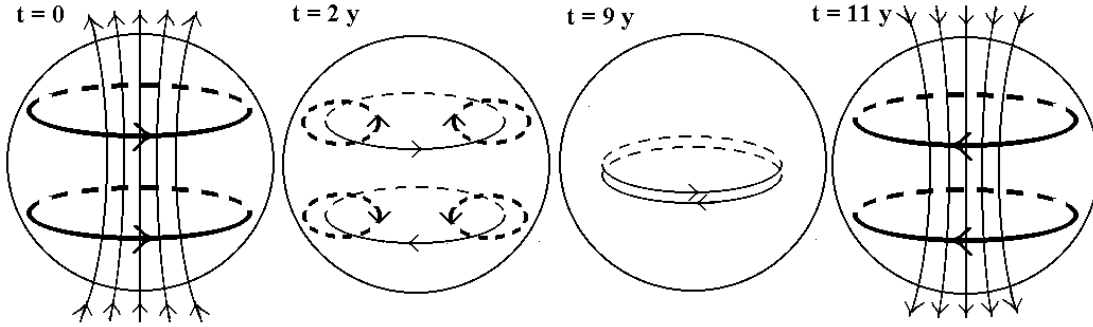


Fig. 2 Magnetic field lines and lines of current (the thick ones) in 11-year solar cycle.

Current sheet formation at new magnetic flux flowing up

Let us consider an active region with two spots (S1 and S2) of different polarity. It produces an arch magnetic configuration. If at $t = 0$ another part of the same magnetic tube is flowing up, the spots S3 and S4 appear. The magnetic fields of spots S2 and S3 are opposite to each other. The CS arises that separates these fields. Magnetic energy accumulated in the course of CS formation can be released during its decay, and solar flare occurs. In the next section of the paper we present the results of MHD simulation of this process.

The CS formation at such magnetic flux flowing up has been reproduced recently in MHD numerical experiment (Podgorny and Podgorny, 1992). Slow field increasing demands long-time calculations in the region with strong magnetic field gradient on the photosphere. Under such conditions a numerical instability develops, because the numerical analogue of $\text{div } \mathbf{B}$ can not be equal to zero exactly, and parasitic currents that disturb the solution appear. As a result, the fact of energy storage has been established, but other effects have not been reproduced. To exclude parasitic current appearance, we have modified the Peresvet code by including the scheme that is conservative with respect to the magnetic flux (Podgorny and Podgorny, 2003).

Numerical experiment

Calculations have been carried out with 241x241 grid. The system of MHD dissipative equations for compressible plasma is solved. The new version of the Peresvet code is used. The finite-difference scheme is absolutely implicit. It is solved by iterations. The implicit code provides high stability of calculations. The numerical technique includes multilevel division of time step in the regions of large gradients. For suppressing numerical instability in such regions a scheme conserving the magnetic flux is developed, which permits to mostly stabilize the instability. Anisotropy of plasma thermal conductivity in the magnetic field is taken into account. Equations considered and numerical methods are described in (Podgorny and Podgorny, 1996).

The size of the active region L_0 is taken as a unit length. The calculation region is $0 \leq x \leq 1, 0 \leq y \leq 1$. The y -axis is directed perpendicular to the solar surface. The magnetic field B_0 above the active region is taken as a unit magnetic field. The units of plasma density ρ_0 and temperature T_0 are taken as initial values, which are supposed to be constant in space. The units of the plasma velocity, time, current density, and dipole moment are taken as $V_0 = V_A = B_0 / \sqrt{4\pi\rho_0}$, V_A being the Alfvén velocity, $t_0 = L_0 / V_0$, $j_0 = cB_0 / (4\pi L_0)$, $M_0 = B_0 L_0^2$.

The magnetic fields of the spots are approximated by vertical dipoles. The positions and directions of the dipoles are shown in Fig. 3. Their parameters are the following: S1 - $X_1=0.1, Y_1=-0.5, \mu_1=0.25$; S2 - $X_2=0.45, Y_2=-0.5, \mu_2=-0.25$; S3 - $X_3=0.78, Y_3=-0.2, \mu_{3\max}=0.25$, and S4 - $X_4=0.85, Y_4=-0.2, \mu_{4\max}=-0.25$. During $\Delta t=50$, dipoles S3 and S4 are linearly increased from 0 to maximum values.

In our calculations the parameters are chosen according to the principle of limited simulation: $\gamma=5/3, \text{Re}_m=10^5, \text{Re}=10^4, \beta=2 \cdot 10^{-5}, \Pi=100, \Pi_B=10^8, G_q=10^{-4}$. The gravitation force can be neglected compared to magnetic and plasma pressure forces: $G_g=0$. For $B_0 = 300$ G, and $n \sim 10^8$ cm/s, the Alfvén velocity is 6×10^9 cm/s. For $L_0 = 10^{10}$ cm the dimensionless unit of time corresponds to 2 s.

Results

The calculations indicate appearance of plasma flux between dipoles S3 and S4. The evolution of magnetic configuration is shown in Fig. 3a-c. The magnetic field lines are stretched inside the sheet, so that $\mathbf{j} \times \mathbf{B} / c$ force is directed upward. Accelerated plasma can be ejected into interplanetary space and produce coronal mass ejection [Podgorny and Podgorny 2002; Dryer, 1996]. The plasma flow exhibits all the features typical for CS dynamics. The upward acceleration results in filament eruption and coronal mass ejection that interacts with the Earth's magnetosphere and leads to substorms. Downward acceleration is not so effective, because it is directed against

magnetic field gradient. It is responsible for hot plasma accumulation at the top of the post-flare loop. The outer part of the loop becomes hotter than its inner part. This feature has been often reported.

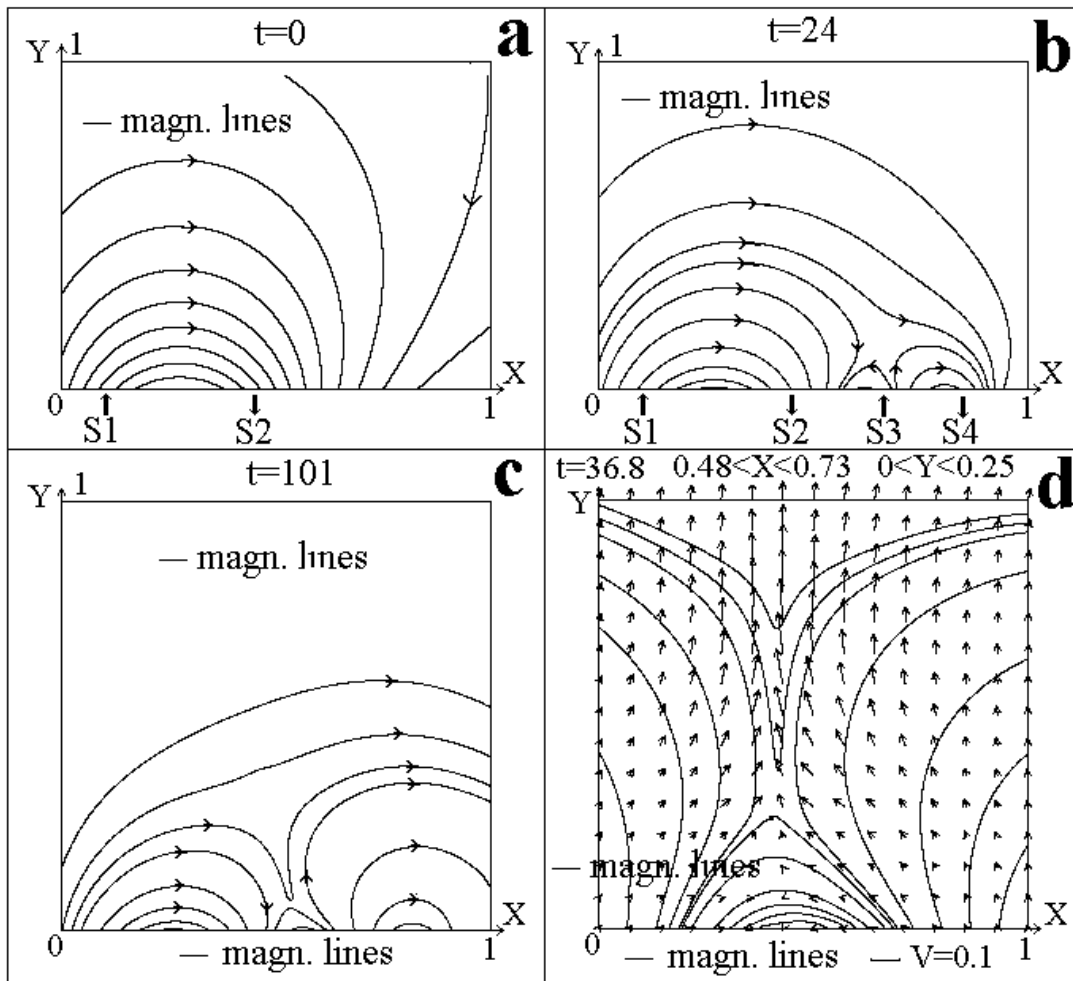


Fig. 3 Magnetic field lines during CS formation.

The velocity vector field in the CS vicinity indicates plasma inflow into the CS. The plasma velocity increases toward the CS under the action of $\mathbf{j} \times \mathbf{B}/c$ force. As a result, the plasma density drops at the both edges of the CS. Such plasma contraction is similar to that associated with the pinch-effect. Inside the CS the force $\mathbf{j} \times \mathbf{B}/c$ accelerates plasma upward and downward. Fast plasma outflow of the CS leads to CS thinning. Isocontours of current density for narrow CS are shown in Fig. 4a, CS thickness being restricted by the step of the grid.

Plasma acceleration inside the CS and its ejection produces further plasma depletion. Arising of such a region reduces plasma inflow. The reduced plasma inflow can not compensate plasma ejection along the CS. The CS thickness drops and instability can develop. As a result, the CS decays, which is accompanied by accumulated energy turning into heat and fast plasma ejection initiating.

The CS is located between the coronal plasma and plasma connected with the flowing-up magnetic flux. In this part of the border the magnetic field changes its direction. Plasma inflow into the CS from the both sides results in a very slow CS displacement. The calculations indicate that the CS rotates and becomes a vertical one.

Plasma density distribution during CS development is very complicated (Fig. 4b). More representative are density isocontours (Fig. 4c). Along with density increase in the CS and density drops from the both sides, a big and broad density maximum in the other part of the border between two plasmas (i.e. old coronal plasma and plasma emerged with the frozen-in flowing-up magnetic field) appears. But in this region the magnetic field is of the same direction, so the current density is very small. This part of the border is a moving extensive front of compressed plasma. MAX marks this front in Fig. 4c. Here density isocontours are shown. The CS position is determined from comparison with magnetic field line distribution (Fig. 4d). After a certain time, the front departs from calculation region. Though this front is not responsible for solar flare energy accumulation, it can produce a rather strong visible effect due to high-density of plasma. Confusion can arise in understanding the mechanism responsible for energy

storage above the active region. By mistake, this high-density front can be considered to provide energy accumulation for the solar flare.

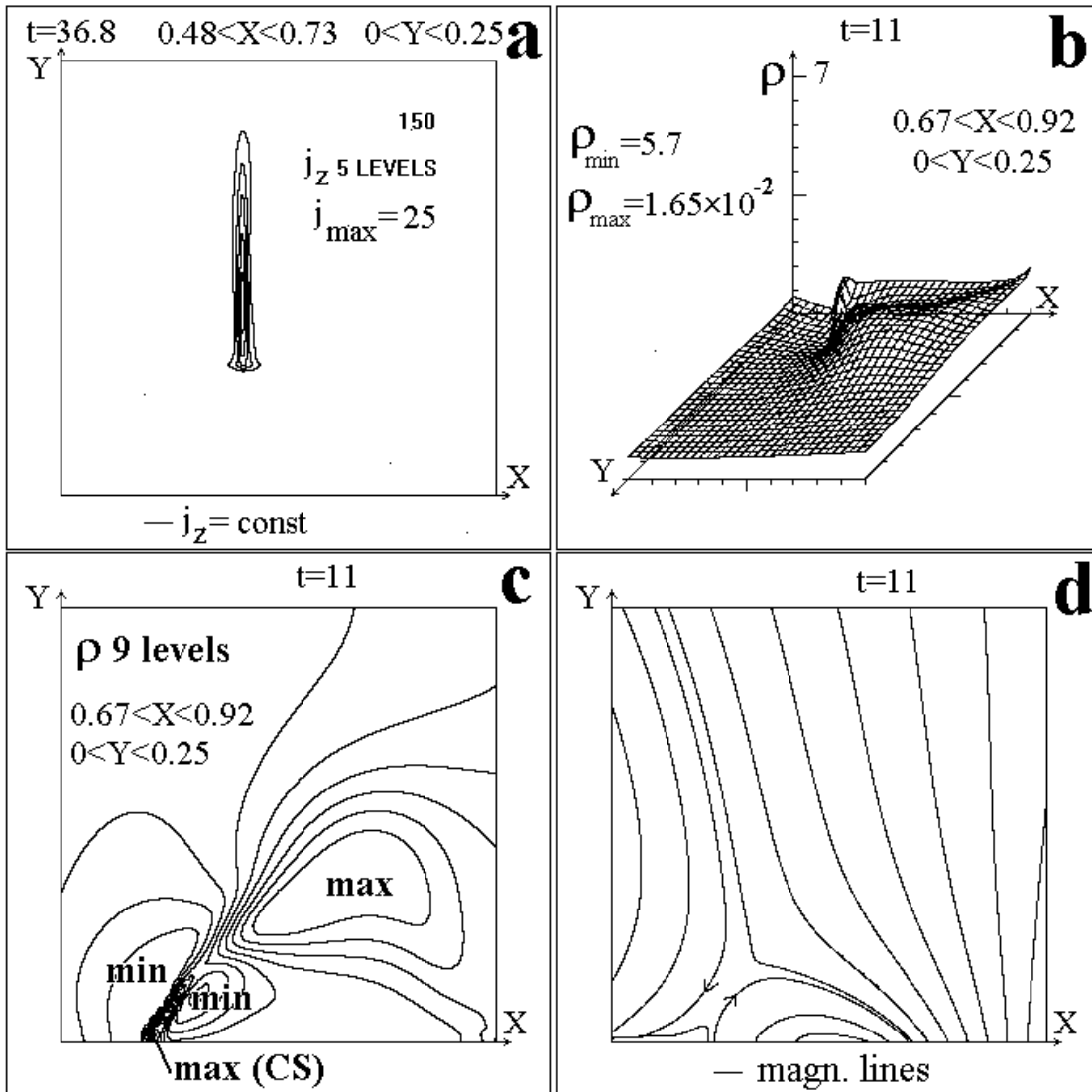


Fig. 4 Distributions of current density, density and magnetic field around the CS

Acknowledgments. The work is supported by the Russian Foundation for Basic Research 01-02-16168 and Astronomiya State Program.

References

- Dryer M. Solar Phys. Comments on the origin of coronal mass ejection. **168**, 421, 1996.
- Podgorny A. I. and Podgorny I. M. Electrodynamical model of the flare and solar flare prognosis. In Solar Driver of Interplanetary and Terrestrial Disturbances. Ed. by K.S. Balasubramaniam, S.L. Keil, R.N. Smartt. ASPCS. V. 95. USA. 1996. P. 66.
- Podgorny A. I. and Podgorny I. M. Solar Phys. A solar flare model including the formation and destruction of the current sheet in the corona. **139**, 125, 1992.
- Podgorny A. I. and Podgorny I. M. Numerical simulation of a solar flare produced by the emergence of new magnetic flux. Astronomy Reports. **45**, 60, 2001.
- Podgorny A. I. and Podgorny I. M. Current sheet decay as a united mechanism of the phenomena associated with a solar flare. Proc. of 25th Annular Seminar. Apatity. 2002. P. 133.
- Podgorny A. I. and Podgorny I. M. Numerical simulation of magnetic field dynamics in solar corona with a scheme that is conservative relative to magnetic flux. Proc. of 26th Annular Seminar. Apatity. 2003. P. 151